Magnetic configurations in 160–520-nm-diameter ferromagnetic rings

F. J. Castaño, C. A. Ross,* A. Eilez,† W. Jung, and C. Frandsen‡
Department of Materials Science and Engineering, Massachusetts Institute of Technology, Cambridge, Massachusetts 02139, USA
(Received 29 August 2003; revised manuscript received 24 November 2003; published 21 April 2004)

The remanent states and hysteretic behavior of thin-film magnetic rings has been investigated experimentally and by micromagnetic modeling. Rings of diameters 160–520 nm, made from Co using lift-off processing, show three distinct remanent states: a vortex state, an ''onion'' state with two head-on walls, and a ''twisted'' state containing a 360° wall. The range of stability of these states varies with ring geometry, with smaller width rings showing higher switching fields and greater variability.

DOI: 10.1103/PhysRevB.69.144421 PACS number(s): 75.75.+a, 75.60.−d, 85.75.−d

I. INTRODUCTION

Magnetic ring-shaped structures have been studied for many years, and macroscopic ferrite rings were used in core memory, an early magnetic data storage device, over fifty years ago.[1] More recently, there has been an upsurge in interest in small thin-film ring-shaped structures (for a review see Ref. 2), motivated in part by their proposed use in magnetic random access memories.[3,4] One appealing feature of thin-film rings is the existence of well-defined remanent states, which could be used to store one or more data bits in each ring. Previous work in micron- and submicron-diameter rings[5–14] has confirmed the existence of distinct ''vortex'' states, where the magnetization runs clockwise or counterclockwise around the ring, and ''onion'' or bidomain states which contain two head-on (180°) walls at opposite ends of a diameter. Lately a third state, called a ''twisted'' state, was identified in submicron rings:[15] this consists of a vortex state containing a 360° wall. Although metastable with respect to the vortex state, the twisted state can exist over a range of fields and at remanence. The twisted state has also recently been proposed for use in magnetic random access memories[4] in which the ring is switched between two twisted states by a small circumferential field.

The behavior of thin-film rings has been explored by several groups as a function of the geometry of the ring. The ring can be parametrized by its outer diameter d, its width w (i.e., the inner diameter is given by d-$2w$), and its thickness t. The majority of experimental work has been carried out on rings with outer diameters from about 500 nm up to several microns,[5–14] but rings with $d=90$ nm and above,[2] $d=180-520$ nm,[15] and octagonal ring shapes with $d=300-800$ nm (Ref. 16) have also been investigated. All the rings exhibit vortex and onion states, and transitions between the states occur by the movement, formation or combination of domain walls. For instance, a vortex state is formed from an onion state by the unpinning of one wall and its movement around the ring until it combines with the other wall. In contrast, twisted states have only been observed in the smaller rings, with diameters of about 500 nm and below.[15] This may be a result of the transverse (Néel) micromagnetic structure of the head-on walls in the onion state in smaller rings, which makes the formation of a metastable 360° wall more likely.

Deep-submicron diameter rings are interesting because of potential applications in high-density devices, and it is therefore important to explore the effect of diameter, width and thickness on ring behavior, in particular the formation and stability of the twisted state. Previous work has shown that the switching field for the onion-vortex transition increases with increasing diameter and film thickness and decreases with increasing width,[12] and that the vortex state is less likely to occur in rings made from thinner films.[2] However, there has not been any detailed investigation of the formation and stability of the twisted state. In this paper, the behavior of Co rings with diameters of 160–520 nm has been investigated as a function of diameter and width. Results are compared with the predictions of a micromagnetic model, which reproduces the existence of vortex, onion, and twisted states.

II. EXPERIMENTAL METHODS

Circular Co rings were fabricated using a Raith-150 electron-beam lithography system[17] and liftoff processing. To avoid edge roughness due to pixellation, the rings were written by scanning the electron-beam along parallel single-pixel circular trajectories. Typically 10 fields with an area of 100×100 μm^2 were written with increasing electron-beam dose. Each of these fields contained nine 8×8 arrays of rings of various dimensions written in a 120 nm thick polymethylmethacrylate layer, spun onto 3″ diameter Si(100) wafers. The resist was developed in a 2:1 solution of isopropyl alcohol and methylisobutylketone at a temperature of 21 °C for 90 sec. After development of the resist, Co (12nm)/ Au (3nm) bilayers were deposited onto the patterns by electron-beam evaporation and a final lift-off step in n-methylpyrrolidone at 120 °C was performed. The rings had a width variation of less than 10 nm. Figure 1 shows a schematic representation of the lithography processing, as well as corresponding scanning electron micrographs (SEM's) after the metal evaporation onto the resist and after the lift-off step. The films were polycrystalline with grain size of order 10 nm. In the present work we investigate circular Co rings with thickness of 12 nm, outer diameters ranging from 160 to 520 nm, and widths of 30 nm and above.

A Zeiss LEO 982 scanning electron microscope with Gemini column was used to image the structures. Magnetic states were determined using a Digital Instruments Nanoscope magnetic force microscope (MFM) with a low-moment tip, typically at 35 nm lift height. MFM tips can

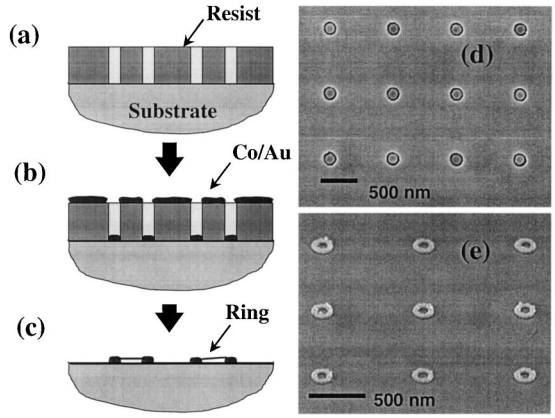

FIG. 1. Schematic representation of the lithographic processing, (a) after the *e*-beam exposure and resist development, (b) after the metal evaporation, and (c) after the lift-off step. Part (d) shows a SEM corresponding to step (b), while (e) corresponds to step (c), in an array of rings with outer diameter of 160 nm and width of 30 nm.

produce significant fringing fields,[18] with components both parallel and perpendicular to the sample surface, but (unlike similarly sized NiFe rings) we found no evidence of tip-induced perturbation of the magnetic states of the Co rings during repeated scans in different directions. This is attributed to the high switching fields of the Co rings. To image, the rings were first saturated in an in-plane field of 10 kOe in an electromagnet, then imaged at remanence. Reverse in-plane fields of different magnitudes and opposite direction to that of the saturating field were then applied and removed, and the rings again imaged at remanence. Remanence images were taken every 70–100 Oe. The reverse in-plane fields were applied *in situ* in the MFM using permanent magnets on an adjustable holder, which were calibrated prior to the experiments. The maximum field that could be applied at the sample was 2500 Oe.

Micromagnetic simulations were performed using two-dimensional OOMMF software, available from NIST (National Institute of Standards and Technology). Circular ring shapes with equivalent dimensions to those of the experimental structures were discretized into $5\,\text{nm}\times 5\,\text{nm}$ square elements. Simulations were also made with 2 nm square elements which gave similar results for switching fields. The model used parameters appropriate for hcp Co (exchange constant $A=3\times10^{-6}$ erg/cm, saturation moment $M_s=1422$ emu/cm^3, and anisotropy $K_1=5.2\times10^6$ erg/cm^3), with a damping coefficient of 1. The direction of the uniaxial anisotropy within each square element was varied randomly in three dimensions to simulate a polycrystalline film. The remanent loops were calculated by equilibrating the magnetic structure at an applied field, then setting the field to zero, equilibrating the magnetization again and then recalculating the remanent magnetization.

III. RESULTS

A. Hysteresis of rings as a function of width and diameter

In all the arrays investigated, MFM indicates that the onion state is present at remanence after saturating the rings at a high field. As the reverse field is increased, the rings typically switch into a twisted state and then into a vortex state, and eventually into a reverse onion state. By appropriate field cycling, all of these states can be imaged at remanence. Figure 2 shows remanent MFM images of onion, twisted and vortex states in rings of different dimensions. Onion states are characterized by dark and light contrast at opposite sides of the ring, the 360° wall in the twisted state shows as a dark-light pair, and the vortex state shows no contrast.

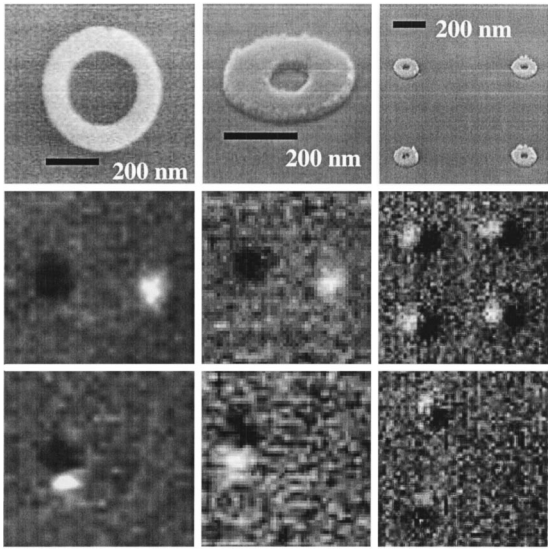

FIG. 2. Top row: SEM images of rings with outer diameters of 500 (left), 360 (middle), and 180 nm (right column). The larger ring is shown in plan view while the other rings are shown tilted. Middle row: MFM remanent images after saturating the sample in a horizontal field of 10 kOe, showing onion states. Bottom row: MFM scans after applying reversing fields of 216, 1000, and 1700 Oe, respectively. The images show twisted states, except for two of the smallest rings which are in the vortex state and therefore show no contrast.

Based on the MFM data, a qualitative remanence loop for an individual ring can be constructed by assigning a remanence of zero for the twisted or vortex state and ±1 for the onion state. An example is shown in Fig. 3 for a 520 nm diameter ring. The zero-moment plateau corresponds to the twisted and vortex states. Two switching fields H_{C1} and H_{C2}, corresponding to the destruction of the onion state and the creation of the reverse onion state, respectively,[2,5–16] can be measured from the remanence loops.

Individual rings show a range of switching fields, so to obtain average values, the collective remanence loop of an array of typically 64 rings was constructed from MFM data. Figure 4 shows how the remanence loops of ring arrays vary with ring diameter and ring width. The fields H_{C1} and H_{C2} both increase with decreasing ring width, as shown in Table I. The dependence of switching fields on diameter is weaker; from the table H_{C1} changes little or increases with increasing diameter, while H_{C2} decreases. This corresponds to a wider zero-remanence plateau for smaller-diameter rings. Additionally, the switching field distribution is greater for narrower rings.

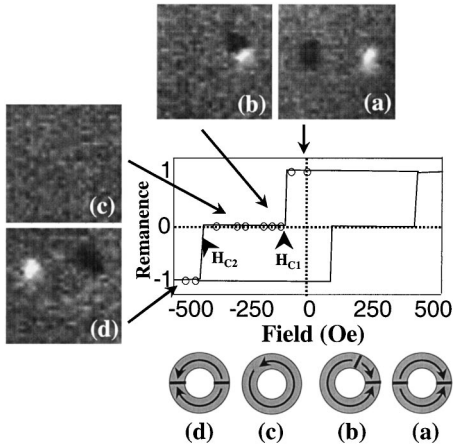

FIG. 3. MFM images of a 520-nm-diameter Co ring showing the evolution of remanent magnetic states in the ring as a function of reverse field, at 0, 108, 179, and 460 Oe. The arrows on the schematic representation of the states indicate the magnetization directions in the ring. (a) Onion state, (b) twisted state, (c) vortex state, (d) reverse onion state. At the center, a remanence loop of the ring has been constructed from these and other MFM images.

Figure 4(b) also shows a minor loop for an array of rings with diameter 360 nm and width 110 nm. After positive saturation, a reverse field of 1370 Oe was applied briefly, which put all of the rings into the vortex state. An increasing positive field was then applied. At a field of H_{C2}, the forward

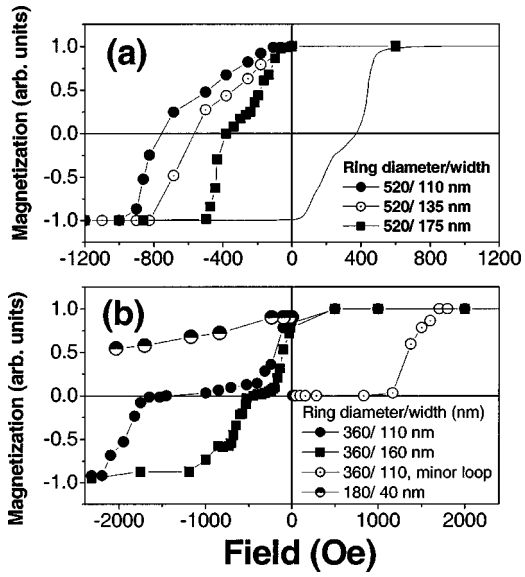

FIG. 4. (a) Remanence loops deduced from MFM data for rings with outer diameter of 520 nm and widths of 110, 135, and 170 nm. The solid lines are provided for clarity and one of the data sets is mirrored to illustrate the entire remanent loop. (b) Remanent hysteresis loops for arrays of rings with outer diameter of 360 nm and widths 110 or 160 nm, and for rings with diameter 180 nm and width 40 nm. Note that the field scale is different from that in (a). A minor remanent loop for the 360 nm diameter, 110 nm wide rings is also shown in which a reverse field of 1370 Oe was applied to generate vortex states, then the field was increased back to positive saturation.

onion state formed, shown in the minor remanence loop. However, in a separate experiment to those undertaken to deduce the minor loop, rings were initially magnetized into twisted states by a smaller reverse field, then an increasing positive field was applied. Average positive fields of 100 and 200 Oe were required to switch twisted states into forwards onion states in nanorings with outer diameter of 520 nm and widths of 170 and 110 nm, respectively. This indicates that only a relatively small field is needed to separate the 360° wall into its two component head-on walls.

Although individual rings behave reproducibly on repeated scans, there is a wide range of behavior between nominally identical rings. An indication of the variation in behavior can be obtained by plotting the range of fields over which a twisted state is observed in the rings of an array. The field ranges for the existence of twisted states of several 520-nm-diameter Co rings are shown in Fig. 5. The twisted state in some rings is found over field ranges of several hundred Oe, while in other rings the state is short lived. The narrowest rings show the most variation in the stability of the twisted states.

B. Morphology of the twisted state

There are four variants of the twisted state depending on which of the two domain walls in the initial onion state moved around the ring and which direction it moved. Four variants observed in a 520-nm diameter ring array are shown in Fig. 6, two with clockwise and two with counterclockwise magnetization directions. The variants occurred with equal frequency in each array. Although it cannot be imaged directly by MFM, once a vortex state forms from a twisted state, the vortex necessarily maintains the magnetization direction of the twisted state that precedes it.

All the twisted states in an array of rings of the same geometry have similar appearance in the MFM images. The arc angle between the domain walls was estimated by measuring the angle θ between the lines joining the center of the ring to the centers of the dark and light MFM contrast, as indicated in Fig. 6(b). For rings with diameters below 200 nm, quantitative measurement was not possible because it is difficult to resolve the positions of the walls with respect to the center of the ring. Results for 360–520 nm diameter rings are shown in Table I, along with the corresponding lengths along the circumference of the ring. The uniformity of this angle for a given ring width and diameter makes it unlikely that creation of the twisted state is controlled by random pinning of the walls. Pinning of walls is seen occasionally, but this gives a different MFM contrast, as exemplified in Figs. 6(e), 6(f). Figure 7 shows the wall angles measured for the twisted, pinned and onion states seen in an array of 520-nm-diameter 170-nm wide rings.

As the ring becomes wider, the angle between the two component head-on walls, and the overall length of the 360° wall in the twisted state decreases. For a constant ring width, the arc length is constant within the error of the measurement. In rare cases, other, more complex states were observed, for instance, a double twisted state consisting of two 360° walls, as well as a triple twisted state containing a 540° wall were reported in 520 nm diameter rings.[15]

TABLE I. Data for the switching fields, the arc angle θ between the positions of maximum contrast in the MFM images of twisted states, and the corresponding length of the feature in the MFM images, for rings of different geometries. Data for the arc angles was based on measuring 5–15 rings of each size.

Ring diameter, nm	Ring width, nm	H_{C1}, Oe	H_{C2}, Oe	Angle θ between walls in the twisted state, deg.	Circumferential length of twisted state, nm
520	170	170	410	33 ± 8	150 ± 36
520	135	330	690	24 ± 6	109 ± 27
520	110	470	850	20 ± 2	91 ± 9
360	160	150	850	39 ± 11	123 ± 35
360	110	240	1900	32 ± 8	100 ± 25

C. Modeling results

Both remanence loops and conventional hysteresis loops were simulated for single rings with dimensions matching those fabricated. Figure 8 shows calculated hysteresis loops for a 360 nm diameter, 110 or 160 nm wide ring. The model reproduces the decrease in switching field with increasing ring width observed experimentally. There is a reasonable quantitative agreement between calculated switching fields and the measured average switching fields, except that the model underestimates H_{C2} for the narrower ring.

Figure 9 shows the calculated remanence loop for the ring of 520 nm diameter and 110 nm width, along with images of the magnetization state of the ring at different stages in the magnetization reversal. Remanence loops display sharper transitions and a lower saturation magnetization than hysteresis loops because the moments relax along the edges of the rings at remanence. The model reproduces the states observed in the MFM images in Fig. 3. In particular, the angle between the midpoints of the head-on domain walls in the twisted state is 25°, which compares well with the measured value of 20 (±2)° from the MFM measurements.

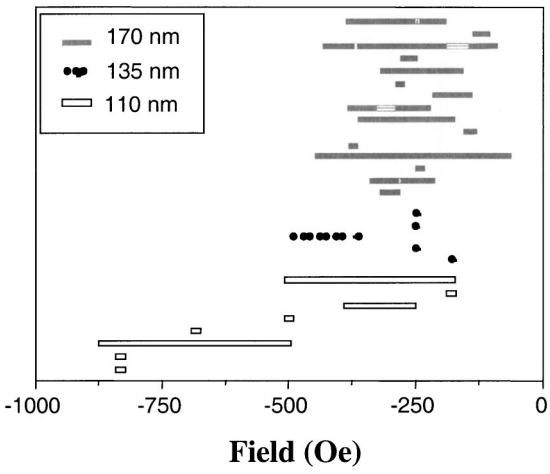

FIG. 5. Field stability ranges for the twisted states seen in three different arrays of 520-nm-diameter Co rings of width 110, 135, and 170 nm, respectively. Each bar represents the range over which the twisted state was seen in an individual ring. Some rings have twisted states that persist over hundreds of Oe while others show a twisted state only over a small field range.

IV. DISCUSSION

The rings in this study are sufficiently narrow and thin that the domain walls have an in-plane, transverse character,[20] and transitions between the magnetic states are accomplished by the creation, movement or annihilation of transverse walls. The switching field H_{C1} represents the field at which the onion state is destroyed by the unpinning and movement of one domain wall, while H_{C2} is the field at which the reverse onion state is formed from a wall-free vortex state by creation of a reverse domain followed by

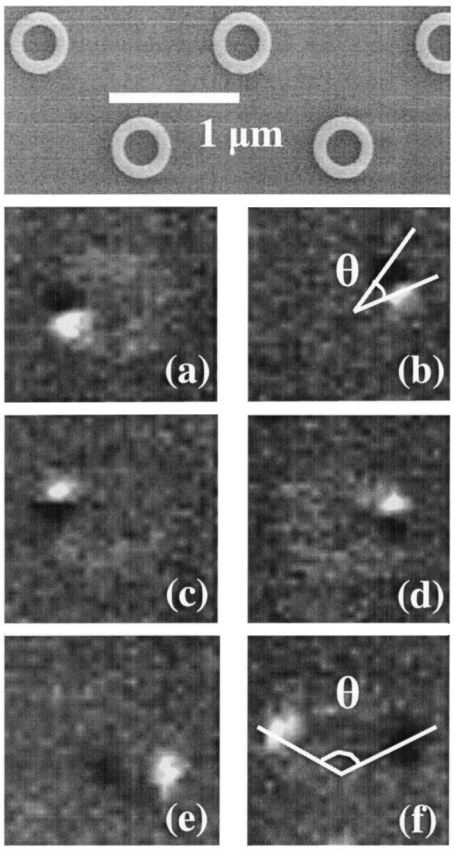

FIG. 6. Top: SEM of several 520 nm diameter, 170 nm wide rings. Below, MFM images (a)–(d) demonstrate four variants of the twisted state seen in four different rings. In (b) the angle θ between the domain walls is defined. (e),(f) Examples of pinned states.

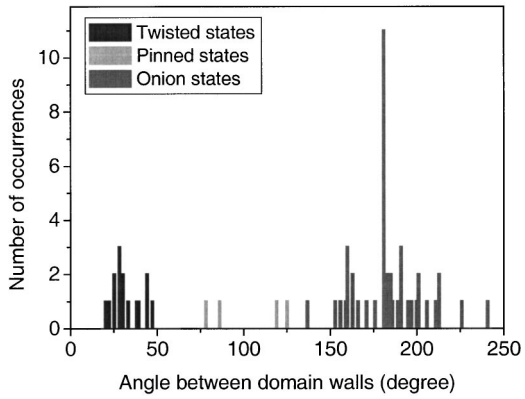

FIG. 7. Histogram of the angles between the domain walls in Co rings, 520 nm in diameter, and 170 nm wide. The distribution of angles between the walls in the twisted state is centered at 33°. The distribution of angles between the walls in the onion state is centered at 180° while the angles in the pinned states vary.

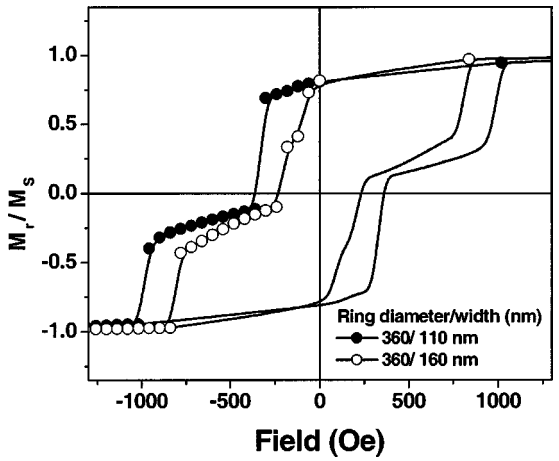

FIG. 8. The simulated hysteresis loop for rings with outer diameter of 360 nm and widths of 110 and 160 nm.

separation of a domain wall pair, at a region of the ring magnetized antiparallel to the applied field. At H_{C1}, the movement of one of the domain walls and its combination with the other to make a 360° wall produces an intermediate metastable twisted state; the twisted state then decomposes into the vortex by the annihilation of the 360° wall at a field intermediate between H_{C1} and H_{C2}. This intermediate field is difficult to measure by conventional magnetometry, because the twisted and vortex states have little or no moment, but the transition can be detected using MFM. Many of the rings in this work showed the onion-twisted-vortex-reverse onion state sequence upon field cycling. In some rings, twisted states were not seen, which indicates either direct transitions between the onion and vortex states, or a small stability range of the twisted state compared to the field step size between measurements. Larger rings, on the micron scale, have not been reported to show twisted states because the 360° wall is unstable in wider structures[15] and easily annihilates to produce a vortex state.

For the ring geometries and film thickness studied here, the ring width is the key parameter in controlling the switching fields, with ring diameter secondary. Both H_{C1} and H_{C2} increase for narrower rings, in agreement with previous results.[2,12,19] H_{C1} is expected to be lower for wider rings where the potential energy landscape in which the wall moves, which is affected by the various microstructural and shape irregularities in the ring, is flatter. The increase in H_{C2} with decreasing width can be attributed to the increasing difficulty for narrower rings in rotating the moments away from the edge of the ring to form a reverse domain.[21] Changes in the switching fields with diameter are less dramatic, especially for wider rings. The data suggest little if any increase in H_{C1}, but a decrease in H_{C2} with increasing diameter. Both H_{C1} and H_{C2} have a wider switching field distribution for smaller and narrower rings. Data from elliptical rings of constant width[19] shows little effect of the radius of curvature on H_{C1}, but H_{C2} is lower when the reverse domain is nucle-

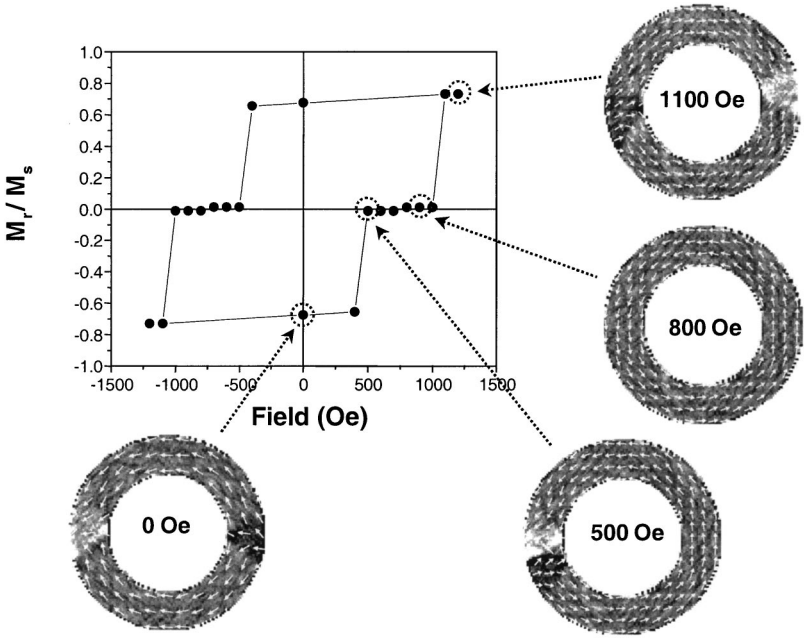

FIG. 9. Simulated remanence loop for a ring structure with outer diameter of 520 nm and width of 110 nm. Images of the different states during magnetization reversal are also depicted for the data points at zero field (onion state), at 500 (twisted state), at 800 (vortex state), and 1100 Oe (reverse onion state).

ated in the more sharply curved section of the ring.

The size of the 360° wall in the ring is governed by competition between exchange energy, which is minimized by a greater separation between the two constituent 180° walls, and magnetostatic attraction between the constituent walls due to their stray fields. The circumferential length of the 360° wall, and the arc angle which it subtends at the center of the ring, therefore depend on the geometry of the ring. The length of the 360° wall is smaller in narrower rings because the total exchange energy is smaller, allowing the walls to approach more closely, while in rings with the same width, the length of the wall along the circumference is similar for different ring diameters. In the example of Fig. 9, the arc angle subtended by the 360° wall is similar to that measured experimentally.

The behavior of rings, as with other lithographically patterned magnetic elements (for example, Ref. 22), shows considerable variability between nominally identical structures. The switching fields for transitions between micromagnetic configurations depend on defects or imperfections in the ring, which affect domain wall generation, pinning, and movement. For a twisted state to form at all, one wall in the onion state must move before the other. In a perfectly symmetrical ring the two walls are expected to move simultaneously and the ring would switch from the onion to reverse onion state without forming intermediate states.[5] In practice, some edge roughness or microstructural irregularity will always break the symmetry of the system. Edge roughness or grain size are more significant in smaller patterned structures, leading to the greater switching field distributions and twisted state stability ranges seen in the smaller and narrower rings. Notably, in a few rings the pinning sites are strong enough to lead to ''pinned states'' with domain walls present at positions different from those characteristic of either onion or twisted states. We observed twisted and pinned states more frequently in rings with greater edge roughness. The twisted state can be reproduced by micromagnetic simulations, because the edge roughness due to the discretization and the random 3D magnetocrystalline anisotropy included in the simulations break the symmetry of the ring.

From the equal probability of appearance of the four variants (Fig. 6) of the twisted states, it appears that the choice of which wall moves first, and which direction it moves around the ring, is random. This choice ultimately determines the circulation direction of the resulting vortex state. By pinning one wall, for instance, with a notch, some control can be imposed over the eventual circulation direction of the vortex,[11] and therefore also over which variant of the preceding twisted state forms.

The minor loop data shows that, as expected, the formation of an onion state from a vortex state occurs at H_{C2} irrespective of the direction of the applied field. A similar result was reported for micron-size rings, in which the onion state formed at the same field H_{C2} for both the minor and major loops.[5] However, if the field direction is instead reversed when the ring is magnetized in a twisted state, the field will act to separate the two 180° walls and recreate the original onion state. Since domain wall nucleation is not required, the recreation of the onion state is expected to occur at a field smaller than H_{C2}. Observations on several rings confirmed this expectation qualitatively.

This work has shown that small rings commonly reverse via intermediate metastable twisted states. The remanent state of a ring could conceivably be chosen from one of eight possibilities (two onion states, four variants of the twisted state, and two different vortex states), or even more complex configurations[15] under appropriate field cycling, provided that pinning sites for the walls can be controlled. This could be useful in devices such as magnetic random access memories, where each ring might store several bits. Readback of the various states could be accomplished by making the rings from magnetoresistive multilayer stacks, and measuring the resistance of the ring under a small perturbing field. A one-bit-per-ring scheme using two twisted states has already been proposed.[4] Even if only the vortex states are used for data storage, to take advantage of their zero stray fields,[3] transitions between them are likely to involve onion or twisted intermediate states, and the switching process will therefore depend on the behavior of domain walls within the rings. As with conventional magnetic random access memory cells made from elongated or tapered elements, the ultimate usefulness of such devices will depend on whether the intrinsic variability between the elements can be controlled. This depends on controlling microstructural inhomogeneity, for example, by using an amorphous or single crystal material, or one with a low magnetocrystalline anisotropy, and reducing edge roughness by improvements in the lithography and patterning processes.

V. CONCLUSIONS

Ferromagnetic thin-film rings with diameters of 160–520 nm, made from 12-nm-thick Co, commonly transform from an onion (bidomain) to a vortex (flux-closed) state via an intermediate metastable twisted state, which contains a 360° wall. Twisted states can be stable over a wide field range, and have a distinctive micromagnetic structure in which the spatial extent of the 360° wall, determined by exchange and magnetostatic interactions, depends on the ring width. Micromagnetic modeling also reproduces the formation of the twisted state during the reversal of a ring. The measured switching fields for transitions between the onion, vortex and twisted states increase with decreasing ring width, vary less strongly with diameter, and show significant switching field distribution. The transitions between the states depend on the movement, creation and annihilation of domain walls and are therefore highly sensitive to microstructural and shape irregularities.

ACKNOWLEDGMENTS

The authors thank Henry I. Smith for the use of facilities at the Nanostructures Laboratory at MIT, and Dario Gil and Feng Zhang for useful discussions. This work was supported by the Cambridge-MIT Institute, the German Academic Exchange Service (DAAD), and the Danish Technical Research Council.

*Electronic address: caross@mit.edu
†Present address: Departamento de Quimica-Fisica, Universidad del Pais Vasco, P.O. Box 644, 48080 Bilbao, Spain.
‡Permanent address: Department of Physics, Technical University of Denmark, Lyngby DK 2800, Denmark.

[1] B. Cullity, *Introduction to Magnetism and Magnetic Materials* (Addison-Wesley, Reading, MA, 1973).
[2] M. Klaui, C. A. F. Vaz, L. Lopez-Diaz, and J. A. C. Bland, J. Phys.: Condens. Matter **15**, R985 (2003).
[3] J. G. Zhu, Y. Zheng, and G. A. Prinz, J. Appl. Phys. **87**, 6668 (2000).
[4] X. Zhu and J. G. Zhu, IEEE Trans. Magn. **39**, 2854 (2003).
[5] J. Rothman, M. Klaui, L. Lopez-Diaz, C. A. F. Vaz, A. Bleloch, J. A. C. Bland, Z. Cui, and R. Speaks, Phys. Rev. Lett. **86**, 1098 (2001).
[6] S. P. Li, W. S. Lew, J. A. C. Bland, M. Natali, A. Lebib, and Y. Chen, J. Appl. Phys. **92**, 7397 (2002).
[7] M. Rahm, J. Raabe, R. Pulwey, J. Biberger, W. Wagscheider, D. Weiss, and C. Meier, J. Appl. Phys. **91**, 7980 (2002).
[8] J. Bekaert, D. Buntinx, C. Van Haesendonck, V. V. Moshchalkov, J. de Boeck, G. Borghs, and V. Metlushko, Appl. Phys. Lett. **81**, 3413 (2002).
[9] C. A. F. Vaz, L. Lopez-Diaz, M. Klaui, J. A. C. Bland, T. L. Monchesky, J. Unguris, and Z. Cui, Phys. Rev. B **67** (14), 140405 (2003).
[10] X. Zhu, P. Grutter, V. Metlushko, and B. Ilic, J. Appl. Phys. **93**, 7059 (2003).
[11] M. Klaui, J. Rothman, L. Lopez-Diaz, C. A. F. Vaz, and J. A. C. Bland, Appl. Phys. Lett. **78**, 3268 (2001).
[12] Y. G. Yoo, M. Klaui, C. A. F. Vaz, L. J. Heyderman, and J. A. C. Bland, Appl. Phys. Lett. **82**, 2470 (2003).
[13] M. Klaui, C. A. F. Vaz, J. A. C. Bland, W. Wernsdorfer, G. Faini, and E. Cambril, Appl. Phys. Lett. **81**, 108 (2002).
[14] X. Zhu, P. Grutter, V. Metlushko, B. Ilic, Y. Hao, F. J. Castaño, S. Haratani, C. A. Ross, B. Vogeli, and H. I. Smith, J. Appl. Phys. **93**, 8540 (2003).
[15] F. J. Castaño, C. A. Ross, C. Frandsen, A. Eilez, D. Gil, H. I. Smith, M. Redjdal, and F. B. Humphrey, Phys. Rev. B **67** (18), 184425 (2003).
[16] S. P. Li, D. Peyrade, M. Natali, A. Lebib, Y. Chen, U. Ebels, L. D. Buda, and K. Ounadjela, Phys. Rev. Lett. **86**, 1102 (2001).
[17] J. G. Goodberlet, J. T. Hastings, and H. I. Smith, J. Vac. Sci. Technol. B **19**, 2499 (2001).
[18] X. Zhu, P. Grutter, V. Metlushko, and B. Ilic, J. Appl. Phys. **91**, 7340 (2002).
[19] F. J. Castaño, C. A. Ross, and A. Eilez, J. Phys. D **36**, 2031 (2003).
[20] R. D. McMichael and M. J. Donahue, IEEE Trans. Magn. **33**, 4167 (1997).
[21] M. Klaui, C. A. F. Vaz, J. A. C. Bland, T. L. Monchesky, B. Unguris, E. Bauer, S. Cherifi, S. Heun, A. Locatelli, L. J. Heyderman, and Z. Cui, Phys. Rev. B **68**, 134426 (2003).
[22] F. J. Castaño, Y. Hao, M. Hwang, C. A. Ross, B. Vögeli, H. I. Smith, and S. Haratani, Appl. Phys. Lett. **79**, 1504 (2001).